Nanoscale

MINIREVIEW

View Article Online
View Journal

Cite this: DOI: 10.1039/d6nr00383d

Chirality-induced spin selectivity in chiral solids

Hiroshi M. Yamamoto [a,b,c]

Chirality-induced spin selectivity (CISS) has emerged as a striking phenomenon in which electron transport through chiral systems generates highly spin-polarized currents, even at room temperature and in the absence of a magnetic field or strong atomic spin-orbit coupling. While CISS has been intensively studied in molecular systems, its microscopic origin remains controversial, partly due to experimental limitations inherent to nanoscale molecules. In this review, the author focuses on CISS in chiral solids and introduces a classification into two categories based on time-reversal symmetry ($\mathcal{T}$): CISS(I), a $\mathcal{T}$-even response associated with collinear current-induced spin polarization, and CISS(II), a $\mathcal{T}$-broken response involving antiparallel spin-pair formation under non-equilibrium conditions. The author further proposes an operational definition based on transport measurements, allowing direct comparison with experiments, including magnetoconductance studies in molecular systems. Recent experiments on chiral metals and superconductors are discussed in this framework, highlighting enhanced spin polarization, nonlocal spin transport, and symmetry conversion between structural and magnetic chirality. These results suggest that chiral solids provide a platform to bridge molecular and condensed-matter perspectives and to explore non-equilibrium spin-chirality coupling.

Received 28th January 2026,
Accepted 27th April 2026

DOI: 10.1039/d6nr00383d

rsc.li/nanoscale

1. Introduction

Chirality-induced spin selectivity (CISS) has recently attracted attention from pure and applied chemistry and physics.[1] CISS can be described as an effect of generating spin-polarized current after the electrons pass through chiral molecules. The spin polarization direction depends on the handedness of the molecule and is parallel or anti-parallel to the current direction (collinear). The most intriguing aspect of CISS is its strength of spin polarization, which is more than 60% even at room temperature without significant atomic spin–orbit coupling (SOC), which was shown clearly in a photoemission electron analysis.[2] Many microscopic mechanisms have been proposed,[3,4] but experimental justification to choose one of those mechanisms is still difficult.

Besides these CISS experiments with organic chiral molecules, it is also expected that chiral metals should become a spin-polarizer, which is known as the Edelstein effect:[5] based on theoretical results in solid-state physics assuming the band structure, chiral conductors can generate spin-polarized current due to a hedgehog-type Fermi surface. The direction of the spin polarization is parallel or antiparallel to the current direction depending on the handedness. In this sense, the symmetrical aspect of CISS is exactly the same as the collinear Edelstein effect. However, its spin polarization is known to be small and is scaled by SOC. Therefore, while the symmetry of CISS is similar to that of the collinear Edelstein effect, the experimentally observed magnitude, nonlocality, and apparent deviation from Onsager reciprocity suggest that additional mechanisms beyond conventional spin-orbit coupling-based descriptions may be involved. In this review, the author will describe the CISS effect in solids where the extent of collinear spin polarization exceeds that of the theoretical limit based on atomic SOC, or the Edelstein effect. An apparent benefit of using chiral solids instead of chiral molecules is that one can utilize both theoretical and experimental methods that are used for solid state physics, such as the Boltzmann equation and spintronics measurements, respectively.

In addition to the above advantage of utilizing solid-state materials, there is another important reason why chiral crystalline conductors are important in understanding CISS. Although CISS can be understood as a simplified concept of a spin filter or spin polarizer, there are several experimental results beyond such an understanding. In particular, it is suggested that a chiral molecule has an antiparallel spin pair on both edges of its body under nonequilibrium conditions.[6] In order to distinguish CISS with an antiparallel spin pair from the original idea described at the beginning, the author would like to categorize CISS experiments into CISS(I) and CISS(II), depending on whether the system follows time-reversal-symmetry ($\mathcal{T}$) invariant or $\mathcal{T}$-broken, respectively. To make the distinction between CISS(I) and CISS(II) operational, it is useful to define them in terms of experimentally measurable responses under $\mathcal{T}$. In transport measurements involving elec-

[a]Institute for Molecular Science, Japan. E-mail: yhiroshi@ims.ac.jp
[b]The Graduate School of Advanced Studies, Japan
[c]Department of Applied Physics, The University of Tokyo, Japan

tric current (I) and magnetization (M), for example, time-reversal operation transforms $(I, M) \rightarrow (-I, -M)$. If the measured response R satisfies $R(I, M) = R(-I, -M)$, the measured response is effectively $\mathcal{T}$-even and corresponds to CISS(I). In contrast, if $R(I, M) \neq R(-I, -M)$, the measured response is $\mathcal{T}$-broken and should be classified as CISS(II). Here, R denotes the resistance for transport measurements. More generally, other rotationally invariant scalar observables may also be used to classify the response, because chirality itself is a rotationally invariant pseudoscalar. This operational definition allows direct comparison with experimental results and provides a unified framework for analyzing both molecular and solid-state CISS phenomena. Note that the antiparallel spin pair belongs to $\mathcal{T}$-broken symmetry as will be discussed later. Therefore, if the system of interest shows CISS(II), symmetry breaking happens not only in the geometry (original sense of chirality) but also in the time domain, which suggests its relevance to the $\mathcal{T}$-odd chirality. Interference among those different types of symmetry may cause confusion, so that step-by-step clarification both in theory and in experiment is required.

Here, the author lists some interesting properties related to the antiparallel spin pair.

1. CISS can be utilized for enantioseparation of chiral molecules by using out-of-plane magnetized ferromagnetic substrates.[6] This phenomenon can be explained by a hypothesis in which an outward/inward antiparallel spin pair is stuck to right-/left-handed molecules, respectively. This spin texture will allow an attracting (repelling) exchange interaction with the magnetic substrate with a given (opposite) magnetization, under free molecular rotation conditions in the liquid (Fig. 1b).

2. One side of the above spin polarization has been detected by anomalous Hall measurements.[7]

3. Handedness specific intermolecular interaction has been calculated.[7]

4. A potential shift due to the exchange interaction between the magnetic substrate and chiral molecules has been observed by Kelvin probe measurements.[8]

5. Large magneto resistance measured in magnetic conductive (mc) AFM can be explained by singlet–triplet energy differences for molecule–substrate interaction with exchange energy. In this case, the selectivity energy can be as large as 30 meV.[8]

6. The (transient) spin polarization on chiral molecules is tightly connected to the molecular orientation on the substrate. If the magnetization direction of the substrate is changed, the molecular orientation will also be changed[9] (strong spin–lattice coupling). It is not clear, however, whether the interaction comes from through-bond coupling or from through-space coupling.

7. The spin polarization on the chiral molecule can also change the magnetization direction of a soft magnet to generate an inter-locked singlet state between the molecule and the magnet.[10] This magnetization relaxes very slowly, implying a transient effect.[11]

The experimental verification of antiparallel spin pair formation in chiral molecules is, however, difficult because the sizes of the molecules are so small that one cannot map out the spin texture inside the molecule. In this sense, materials with crystallographic chirality may provide another chance to detect local spin polarization inside the chiral body because the size of the crystals is macroscopic. In this short review, the author describes the experiments related to the CISS(I) and CISS(II) effects in solids and tries to compare them with molecular CISS.

Before getting into the experimental results, let the author clarify the symmetrical aspects of chiral structures and spin textures, the latter of which are connected to dynamical chirality proposed by Barron.[12] Such a classification is important because it can provide us with criteria for distinguishing the chiral effect from other achiral effects in analyzing the internal mechanism of CISS(I) and CISS(II).

When dealing with the symmetry of physical fields and base functions, it becomes necessary to discuss the evenness or oddness not only of mirror-symmetry but also of time-reversal symmetry.[13] This is because quantities such as magnetic

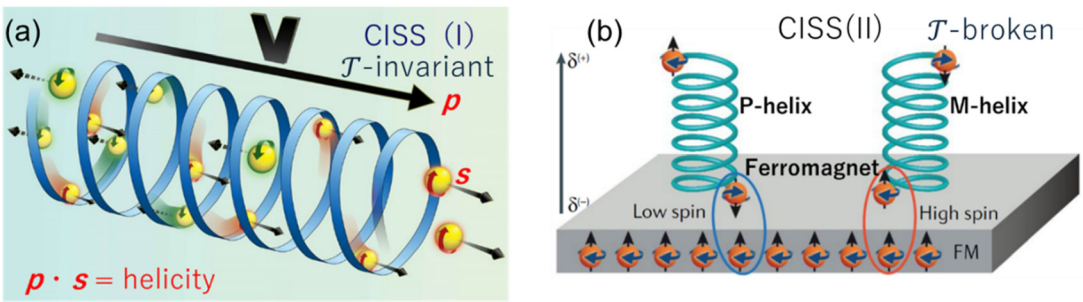

Fig. 1 The conceptual images of (a) CISS(I) and (b) CISS(II). After time-reversal ($\mathcal{T}$), the system remains the same in CISS(I), but the situation becomes opposite for CISS(II): in the right panel, the *P*-helix has an outward spin pair that forms singlet-spins with a ferromagnetic substrate. These outward spins on the *P*-helix will become inward spins and the up-spin in the substrate will become a down-spin after time-reversal. Then, the down-spin polarized substrate will also have singlet-exchange interaction with the *P*-helix, which contradicts with experiment. Therefore, $\mathcal{T}$ is broken in the right panel. Note that the ferromagnetic substrate is used only for detecting the $\mathcal{T}$-breaking of the chiral molecule, so $\mathcal{T}$-breaking of the substrate is not essential in this discussion. (a) is adapted from ref. 1c with permission from ACS, copyright 2016. (b) is adapted from ref. 6 with permission from AAAS, copyright 2018.

fields and spins (time-reversal-odd axial vectors) and quantities involving time derivatives like momentum p change the direction under time-reversal operations (odd symmetry), necessitating differentiation from physical quantities unrelated to time-reversal, such as electric fields E (even symmetry). Importantly, chirality is also a $\mathcal{T}$-even quantity like mass. Another point to be cautious about when dealing with axial vectors is the difference between spatial inversion operations ($\mathcal{P}$) and mirror operations (σ). Axial vectors do not change sign under $\mathcal{P}$ (even) but do have two different symmetries under σ. Specifically, they change sign (odd) when the mirror is parallel to the vector's direction but do not change sign (even) when the mirror is perpendicular to the vector's direction (Fig. 2(a)). The concept of multipoles as symmetry-adapted bases is very effective in treating these properties in a unified manner, and it is now understood that the electric toroidal monopole G_0 represents chirality.[13,14] This is essentially the same with Barron's idea of $\mathcal{T}$-even pseudoscalar,[12] but provides its quantum mechanical version.

As shown in Fig. 2 left panel, localized spin itself is not chiral. On the other hand, moving electrons with collinear spin orientation, which can be called helical, are chiral. Helical electrons that are spin-polarized parallel or antiparallel to their velocity result in a finite $p{\cdot}s$, where p is a linear momentum. Since $p{\cdot}s$ is a $\mathcal{T}$-even pseudoscalar, it can be called electronic chirality (Fig. 2(b)) (the relationship between γ5 in the Dirac equation and helicity is described in ref. 14). The CISS effect is a phenomenon in which molecular chirality G_0 (1) induces electronic chirality $p{\cdot}s$ (G_0 (2): also called helicity). Note that $p{\cdot}s$ is a $\mathcal{T}$-even quantity. In the photoelectron experiments in ref. 2, spin-polarized "unbound electrons[3]" are observed, and this is known as a typical example of the CISS effect. Can other CISS effect experiments be explained with the same concept? In fact, the CISS effect in "bound electrons[3]" in solids is considered to be less straightforward. Specifically, Naaman *et al.*[7,8] has proposed that the electronic spin in molecules feels chirality rather as an antiparallel spin pair, as discovered by enantioselectivity at the magnet surface magnetized in the out-of-plane direction.

Magnetoconductance measurements in chiral molecular systems, particularly those using magnetic conductive AFM (mc-AFM), have reported large resistance asymmetries depending on both current direction and magnetization.[1] In many cases, it is found that the resistance follows $R(+I, +M) \neq R(-I, -M)$ for a given chirality. Since such behavior is not invariant under time-reversal operation, the measured response is $\mathcal{T}$-broken. Accordingly, the exchange interaction (J) between a given chiral molecule and a magnetic substrate violates $\mathcal{T}$ as $J(+M) \neq J(-M)$, as shown in Fig. 1(b), so that chiral discrimination is possible. Within the present classification, they can therefore be interpreted as manifestations of CISS(II), rather than simple spin filtering corresponding to CISS(I). This viewpoint suggests that the large magnetoresistance observed in molecular systems may originate from non-equilibrium processes associated with antiparallel spin-pair formation.

Let us focus on the antiparallel spin pair, which can be regarded as a magnetic monopole (M_0) in multipole language.[13] M_0 is a divergence (source or sink as enantiomers) of magnetic flux. M_0 is odd with respect to all σ and since the enantiomers (inward/outward spin pair) are not superimposable by rotation, as shown in Fig. 3, it is chiral in the sense defined by Lord Kelvin. However, since M_0 is also odd with respect to $\mathcal{T}$, it can be called falsely chiral in Barron's terms.[12] Then an interesting question here is whether there is any relationship between this false chirality M_0 and true chirality G_0. Barron discussed that there is no lifting of G_0 energy degeneracy in equilibrium by M_0. If M_0 can be generated from G_0, however, M_0 can be a function of G_0, namely $M_0(G_0)$, in a special situation. Enantio-separation experiments by CISS imply that there seems such a connection between them, because otherwise it is impossible to discriminate enantiomers by the magnet surface. The antiparallel spin pair appearing in the CISS effect of bound electrons is a good example of M_0, and it has been found that large magnetoresistance effects and chiral resolution are realized because the outward and inward spin pairs are coupled with right-handed and left-handed molecules, respectively.[8] In other words, it seems possible to realize a one-to-one relationship between the signs of G_0 and M_0, so that M_0 represents molecular chirality under certain conditions $M_0(G_0) = -M_0(-G_0)$ (from theoretical consideration, nonlinear and non-equilibrium conditions are implied[15]). The CISS effect in bound electrons utilizes struc-

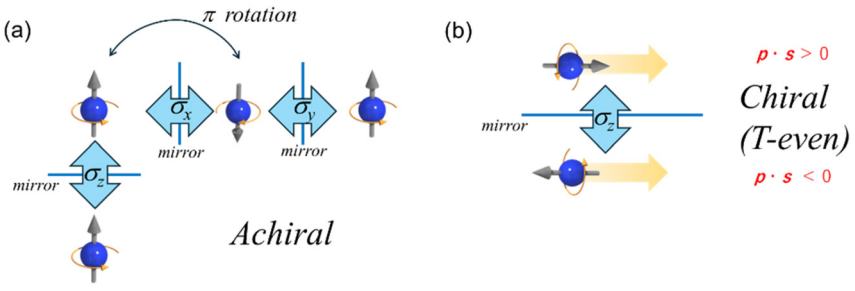

Fig. 2 Electron spin and chirality. (a) The spin of a localized electron reverses under a mirror operation parallel to the spin but returns to the original state upon 180° rotation. (b) Electrons with spin polarization collinear with momentum reverse the sign of helicity under a mirror operation and never return to the original state, no matter how much they rotate.

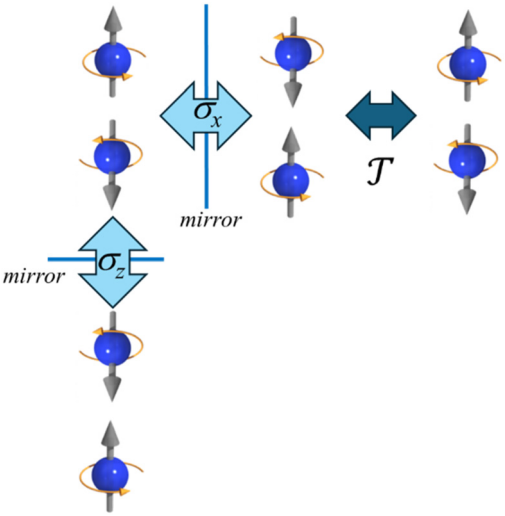

Fig. 3 Conceptual diagram of antiparallel spin pairs. Mirror operations on the *x*- or *z*-direction with respect to outward antiparallel spin pairs result in inward antiparallel spin pairs, which are not superimposable with the original structure. Importantly, this conversion between enantiomers can also be achieved by time-reversal operations $\mathcal{T}$.

tural chirality information after passing through M_0. Can this coupling be visualized experimentally? (For theoretical coupling between G_0 and M_0, see ref. 13–15.) Experiments such as chiral resolution using magnetic substrates,[6] giant magnetoresistance in mc-AFM,[16] and spin polarization detection by the Hall effect,[7] all of which are $\mathcal{T}$-broken phenomena, are known, but these can be considered as indirect evidence at best. Therefore, the author and his collaborators attempted to achieve a macroscopic realization of the situation likely occurring in chiral molecules by using a superconducting material with a chiral crystal structure. The advantage of using a chiral superconductor is that the size of the sample is much larger than that of the molecules, which allows one to map out the spin distribution inside the material while keeping a quantum coherence. As a result, the present experiments provide evidence suggesting that the chirality of the crystal and the chirality of antiparallel spin pairs are indeed coupled.[17] At the same time, our studies showed both CISS(I) and CISS(II) in metallic and superconducting solid systems, respectively. Here the author will introduce these two recent findings from the next section. Both results suggest that chiral solids can indeed exhibit the CISS effect both in $\mathcal{T}$-even and $\mathcal{T}$-broken chirality forms, which correspond to CISS(I) and CISS(II), respectively. Additional advantage of using such solid-state materials is that one can use spintronics in the measurements which correspond to CISS(I) and CISS(II). These results will provide considerable interest in future developments.

From a theoretical standpoint, it is important to distinguish between spin polarization and magnetoconductance. Magnetoconductance is not a direct measure of spin polarization and may include contributions from lattice, vibration, or non-equilibrium charge redistribution. In linear response, Onsager reciprocity requires that transport coefficients are invariant under time-reversal symmetry. Therefore, the observation of magnetoconductance that violates $R(I, M) = R(-I, -M)$ implies that the system is driven out of equilibrium.[4] In this sense, many CISS-related transport experiments, particularly those involving ferromagnetic electrodes, should be regarded as intrinsically non-equilibrium phenomena, which naturally connect to the CISS(II) category. Regarding the chiral separation, in addition to the normal van der Waals and electrostatic interactions, a chirality-dependent exchange interaction J seems to exist as previously mentioned. This interaction satisfies $J(G_0, M) = -J(-G_0, M)$ when handedness is inverted, and $J(G_0, M) = -J(G_0, -M)$ when magnetization is inverted. This may be another important symmetrical aspect of CISS(II).

2. CISS in a chiral metal – CISS(I) in a chiral solid

In the above, the author has discussed some advantages of exploring the CISS effect in chiral solids. As a first example, CISS(I) or the current-induced spin polarization in chiral conductors will be discussed. Historically speaking, current-induced magnetization in a chiral material was measured in chiral tellurium as an optical rotation proportional to the applied current.[18] Recently, NMR measurement was also performed for tellurium under direct current.[19] However, these experiments can be well explained by spin- and orbital-polarized band transport, which means that the effect is the same as the collinear Edelstein effect. Important difference between those previous experiments and our experiments on CISS[20,21] is the quantified strength of the spin polarization that exceeds SOC. At the same time, Onsager reciprocity and non-locality of CISS were detected. Namely, by using spintronics technologies such as the spin Hall effect (SHE) and its inverse effect (ISHE) as well as SQUID magnetometer measurement, it has been shown that chiral $CrNb_3S_6$ can exhibit current-induced spin polarization (CISS(I)) that exceeds the SOC-limit and its inverse effect (iCISS).

$CrNb_3S_6$ is a paramagnetic material with both localized and itinerant electrons' spins at room temperature. The localized moment is known to show Curie–Weiss-type temperature dependency, which exhibits a magnetic phase transition to form helical order at about 130 K. As shown in Fig. 4, a tungsten electrode was attached to a $CrNb_3S_6$ microstrip. It can absorb the current-induced spin polarization in $CrNb_3S_6$ into the vertical direction and generate transverse voltage due to the ISHE.[20] When the chirality of $CrNb_3S_6$ was inverted, spin polarization was also inverted, which is consistent with CISS(I) or Edelstein effect symmetry. The transverse resistance R was proportional to the applied current so that the system satisfies $R(I) = R(-I)$, which is the manifestation of $\mathcal{T}$-invariance (R is V_{yx}/I in this case). iCISS was also measured by inducing spin current inside the tungsten electrode: the spin current injected from the tungsten electrode to $CrNb_3S_6$ generated a voltage inside $CrNb_3S_6$ along the spin direction. With these experiments, it has become possible to create spintronics devices

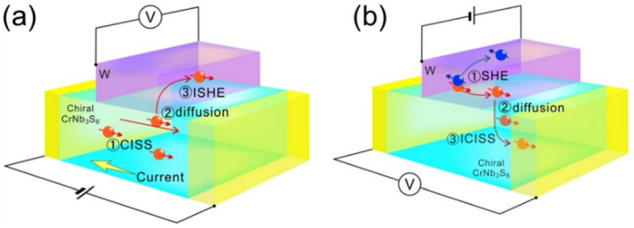

Fig. 4 Schematic diagram of the spintronics device composed of $CrNb_3S_6$ and a tungsten (W) electrode. In CISS mode (a), a bias current was applied to $CrNb_3S_6$ and the polarized spin diffused into W to generate a transverse voltage by the ISHE. On the other hand, in iCISS mode (b), a spin polarization was created by the SHE in W and diffused into $CrNb_3S_6$ to induce a voltaic effect by iCISS. The observed spin signal satisfies Onsager reciprocity and corresponds to a $\mathcal{T}$-even response, consistent with CISS(I). The output voltage was linear to the input current in both cases.

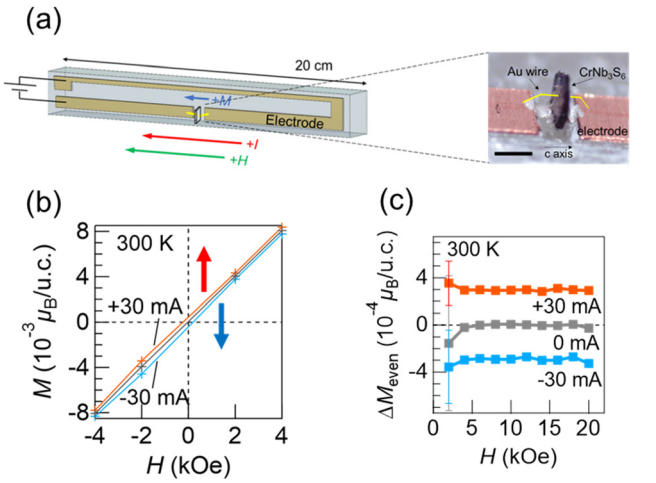

Fig. 5 (a) Experimental setup for SQUID measurement under an applied current. The stray Oersted field was kept small by the elongated electrode configuration. (b) Magnetization curve with and without the applied current. (c) Current induced magnetization measured in various magnetic fields.

based on bulk CISS. What was even more surprising in this experiment was that the chiral material can show a non-local spin signal in a very far distance compared to other systems. When the tungsten electrode is located in a separated area far from the bias current, it could still detect spin polarization. Although the mechanism of this long-distance non-local spin polarization is yet to be explored, it will also provide an important clue for the understanding of CISS in future.

As mentioned above, an important difference between the Edelstein effect and the CISS effect is the magnitude of spin polarization. If the spin polarization remains within the calculated limit for the Edelstein effect, it should be mentioned as the Edelstein effect. In order to clarify this point for $CrNb_3S_6$, we have also performed SQUID measurement, which allows us to estimate the absolute value of spin polarization.[21] In order to estimate the absolute value of the polarization, the author and coworkers have again employed $CrNb_3S_6$ and have measured the magnetic moment directly with a SQUID magnetometer when a current is applied. Fig. 5a shows the experimental setup of the sample loading. The current is applied along the *c* axis of $CrNb_3S_6$, which is the 6_3 screw axis of the material. The crystal is not enantiopure, but it has finite *enantio* excess. As an electrical current is also known to generate a stray Oersted field, which can be mixed with the magnetization signal, the setup should be carefully designed. Such a field can be, however, minimized by placing the turn-around point of the current as far as possible from the sample.

The current-induced magnetization was measured by applying plus/minus 30 mA d.c. into the $CrNb_3S_6$ single-crystal while *M*–*H* curves were measured, as shown in Fig. 5b. In addition to the paramagnetic response, there was a finite zero-field section in magnetization that depends on the current direction. In order to exclude the heating effect, which changes the slope of the *M*–*H* curve, and to properly evaluate the current-induced value, even part of the magnetization shift was calculated as $\Delta M_{even} = [M(+H) + M(-H)]/2$. As shown in Fig. 5c, ΔM_{even} was independent of the magnetic field, which was consistent with the CISS effect. The estimated spin polarization at 30 mA was about $3 \times 10^{-4} \mu_B$ per unit cell. This value far exceeds the number of electrons that are shifted at the Fermi surface by the current bias (the density is about 2×10^{-9} per unit cell), corresponding to an apparent polarization efficiency of 10^7% when normalized with the number of current-biased carriers. The value exceeding 100% does not correspond to the polarization of individual carriers but rather reflects collective amplification of spin angular momentum *via* exchange interactions. This effect cannot be explained by the Edelstein effect because the Edelstein effect is spin polarization of biased electrons. It seems that spin-polarized electrons transfer their spin angular momentum to surrounding electrons by exchange interactions while their polarization is recovered repeatedly by CISS. This enhancement by 10^5 times may come from an enhanced SOC specific to chiral systems, but the detailed mechanism is unknown. The current-induced magnetization ΔM_{even} was proportional to the applied current and was independent of the external magnetic field, again confirming the $\mathcal{T}$-even character of the response. (The current-induced magnetic susceptibility $\chi(\Delta M_{even}, I)$ was constant and therefore the response was $\mathcal{T}$-invariant.) Temperature dependency showed moderate variation, which was similar to Pauli paramagnetic response rather than Curie–Weiss-type susceptibility (Fig. 6). Although $CrNb_3S_6$ has both itinerant and localized electrons, the former seem to be responsible for this spin polarization. It is also worth noting that the temperature dependence of the CISS effect differs between molecular systems and chiral solids. In many molecular experiments, the CISS signal has been reported to increase with temperature, whereas in the present solid-state systems, the effect shows relatively weak temperature dependence. This difference may originate from the underlying transport mechanisms. In molecular systems, charge transport is often dominated by hopping processes and localized states, where thermal activation plays

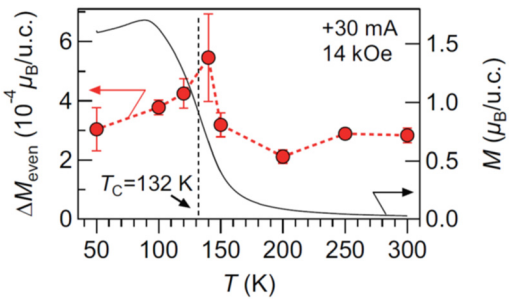

Fig. 6 Temperature dependency of the current-induced magnetization (red dots). The solid black line shows the magnetic susceptibility of a bulk crystal without current.

an important role. In contrast, in chiral solids, itinerant electrons contribute to transport, and the spin response may be governed by band-like mechanisms that are less sensitive to temperature. Although a unified understanding is still lacking, this contrast suggests that the temperature dependence of CISS should be discussed separately for hopping-dominated molecular transport and band-like transport in chiral solids.

3. CISS in a chiral superconductor – CISS(II) in a chiral solid

In the introduction, the author has discussed $\mathcal{T}$-odd chirality made of a spin cluster. The author also pointed out that there seems to be a one-to-one correspondence between the signs of G_0 ($\mathcal{T}$-even chirality) and M_0 ($\mathcal{T}$-odd chirality) in CISS. In this section, the author will show experimental evidence for the conversion from G_0 (crystal chirality) to M_0 (antiparallel spin pair) by using an organic superconductor with a chiral crystal structure. Our research group focused on the chiral organic superconductor κ-(BEDT-TTF)$_2$Cu(NCS)$_2$ (hereafter referred to as κ-NCS). κ-NCS is a quasi-two-dimensional superconductor with stacked superconducting layers. Although the individual ions are not chiral, the combination of BEDT-TTF cations and Cu(NCS)$_2$ anions creates chirality, and κ-NCS belongs to the three-dimensional space group $P2_1$. As a result, there exist mirror-image left- and right-handed crystal structures. The handedness of the crystal structure was determined using a CD microscope, as shown in Fig. 7.

A schematic diagram of the measurement setup is shown in Fig. 7a. First, we prepared magnetic (nickel) and non-magnetic (gold) electrodes on a substrate. Then an electrochemically grown thin single crystal of κ-NCS was laminated onto the substrate. After checking the handedness using a CD microscope, it turned out that thin κ-NCS tends to form a right-handed single domain. The twofold helical axis of κ-NCS, or the *b*-axis, was aligned along the *y*-axis, as shown in Fig. 7a, and an alternating current was applied between the electrodes. If spin accumulation due to the CISS effect occurs near the nickel/κ-NCS interface, a d.c. potential difference V should arise at the interface, because CISS is a spin rectification effect.

Fig. 7d shows V as a function of the applied magnetic field H. The system temperature was set near the superconducting transition point of the κ-NCS thin-film crystal, around 7.4 K. V was antisymmetric and non-linear with respect to H, and its H dependence matched well with the H dependence of nickel magnetization. This result corresponded to the situation where the nickel magnetization was reversed by H while keeping the spin polarization direction of the CISS effect constant. When the obtained V was compared to that calculated for the Edelstein effect, it turned out that SOC enhancement by 1000 times took place in this case, which is again a signature of CISS.

Next, by measuring V at various magnetic field angles θ, we determined the spin polarization direction of the CISS effect. Here, θ is the magnetic field angle within the conducting plane (*bc* plane) of κ-NCS measured from the twofold helical axis *b* (see Fig. 7a). The antisymmetrized measured voltage $V_{odd} = [V(+5\ \text{kOe}) - V(-5\ \text{kOe})]/2$ vanishes at a certain magnetic field angle and reverses sign at that point. Considering that V disappears when the nickel magnetization and the CISS effect spin polarization are orthogonal and that the majority spin angular momentum on the Fermi surface of nickel is parallel

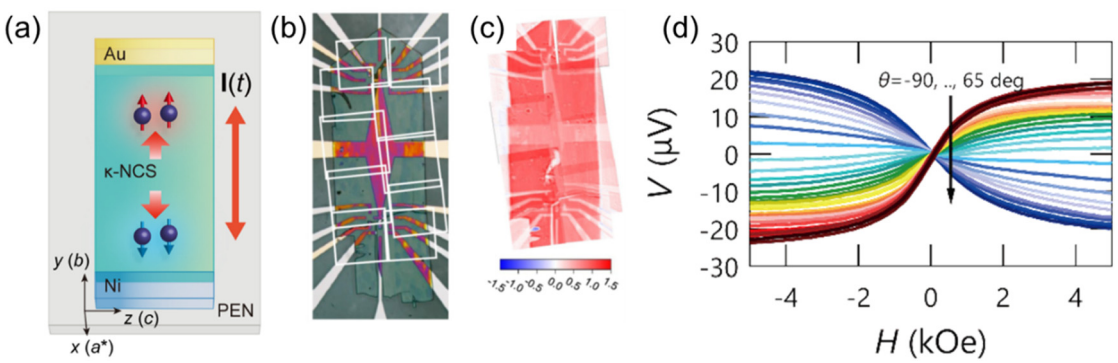

Fig. 7 (a) Schematic of the CISS experiment with κ-NCS. AC bias was applied in the *b* axis direction to drive the spin rectification. (b) Microscopic image of the device. The white squares show the CD microscope fields of view. (c) CD microscopy image of the crystal, which shows a right-handed structure in the entire crystal. The field of view is identical to Fig. 1b. (d) Angle-dependent voltage V across the nickel and gold electrodes. Magnetization M of the nickel electrode was rotated by the external magnetic field H, whose angle to the *y* axis is defined by θ.

to the external magnetic field, the spin polarization direction can be calculated. We conducted similar analyses on the upper and lower ends of the κ-NCS thin-film crystal to obtain the spatial distribution of the spin polarization direction. The spin polarization directions within the same (upper or lower) half of the thin-film crystal were almost the same. However, when comparing spin directions between the upper and lower ends, they were reversed. This was also confirmed by using nonlocal detection, where the excitation and detection terminals were spatially separated (Fig. 8). This result is consistent with macroscopic antiparallel spin pairs that represent $\mathcal{T}$-odd chirality, suggesting the existence of the CISS(II) effect. Notably, the outward/inward spins are related to the right/left-handedness of the crystal domains that are excited by a.c. (Fig. 8a and b) when the crystal has two domains with opposite handedness. This means that G_0 to M_0 conversion took place in the system (Fig. 9). In this way, these experiments successfully visualized the hypothesized antiparallel spin pair for the first time. An important thing here is that the sign of the antiparallel spin pair is rooted in the chirality of the crystal.

Our experimental results indicate that κ-NCS behaves as if it were a single chiral molecule, which has antiparallel spin pairs whose outward/inward spin enantiomers are associated with the right/left handedness of molecular chirality. If such a

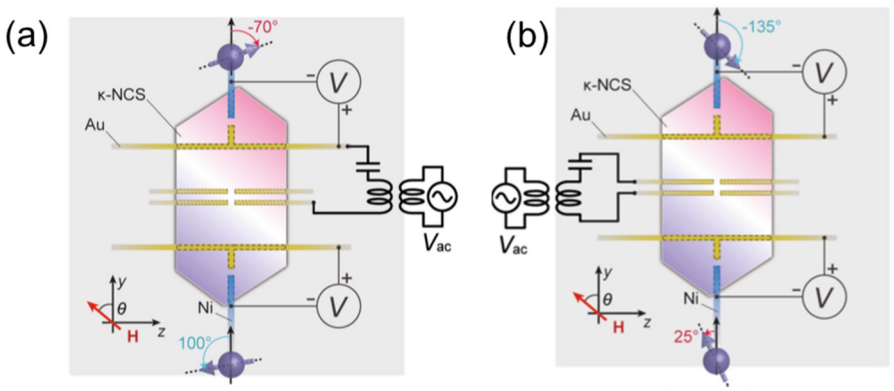

Fig. 8 Schematic diagram of the non-local spin measurement with a Janus-type crystal composed of a right-handed domain (red area) and a left-handed domain (light blue area). (a) The right-handed domain was excited by AC and the outward spin pair was detected. (b) The left-handed domain was excited by AC and the inward spin pair was observed. The opposite spin directions observed at opposite edges indicate a $\mathcal{T}$-odd spin configuration, corresponding to CISS(II).

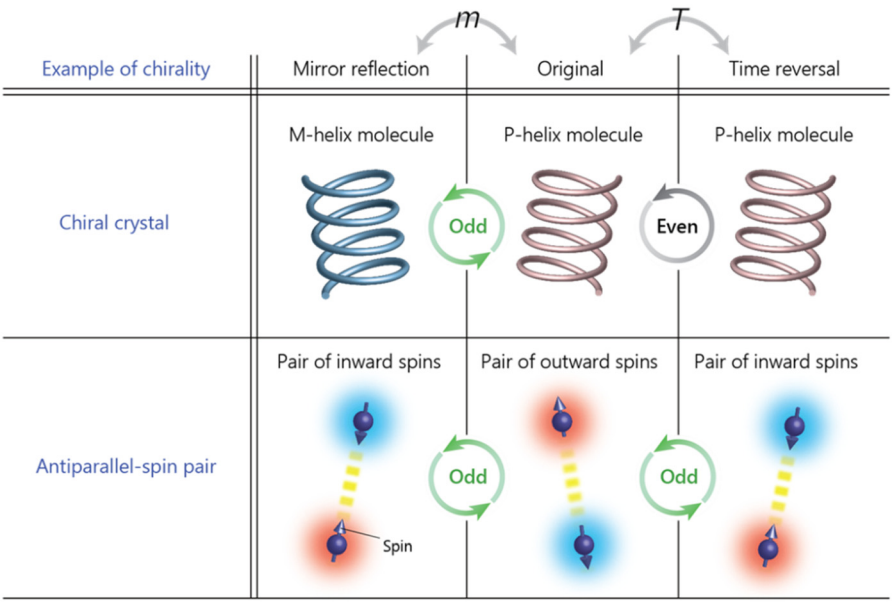

Fig. 9 A table summarizing the relationship between $\mathcal{T}$-even chirality and $\mathcal{T}$-odd chirality. The chirality of the crystal can be inverted only by mirror operation, not by time-reversal, which means that it is $\mathcal{T}$-even chiral. The enantiomer of the antiparallel spin pair, on the other hand, can be inverted both by mirror operation and by time-reversal, which means that it is $\mathcal{T}$-odd chiral. An important point here is that those two different chiralities are connected to each other in reality, by selecting only one type of combination (in the κ-NCS case, the right-handed domain is connected to the outward spin pair, not with the inward spin pair).

spin texture arises in the chiral molecules, chiral separation between right and left molecules at the magnet surface seems possible.[6] Additionally, the experimental result that a chiral antiparallel spin pair is generated from alternating current supports a mechanism in which a helical spin current of G_0 first appears and then is converted to an M_0 antiparallel spin pair at the crystal edges. In addition, by using two enantiomeric domains, it is confirmed that $M_0(G_0) = -M_0(-G_0)$. As Barron correctly pointed out, it is impossible to interconvert $\mathcal{T}$-odd enantiomorphism to the molecular chirality in equilibrium and *vice versa*.[12] Under non-equilibrium conditions, however, such coupling becomes possible, which is supported by the antiparallel spin pairs of the CISS effect, as we currently understand. The author also comments on the handedness dependency of the system in CISS(II). In the case of CISS(II), the response is likely to be restored when both time and the handedness of the chiral molecule are inverted. This kind of phenomenon can be described as $R(G_0, I, M) = R(-G_0, -I, -M)$ in mc-AFM and $J(G_0, M) = J(-G_0, -M)$ in chiral separation. The experimental results seem to support such a relationship in general. This is another reason why M_0 is relevant to CISS(II) because M_0 after $\mathcal{T}$ and $\mathcal{P}$ operations returns to the same $\mathcal{PT}$-symmetry. The author hopes that this study contributes to the elucidation of the mechanism and the construction of a theory for the CISS effect that can be experimentally tested in future.

Another interesting finding in κ-NCS is that it also shows a $\mathcal{T}$-even chiral effect, namely electric magnetochiral anisotropy (eMChA), under an external magnetic field (B). In the case of eMChA, a chiral field $I{\cdot}B$ is created by collinear arrangement of an electric current and a magnetic field, to interact with the chirality of the lattice.[22] Since $I{\cdot}B$ is a $\mathcal{T}$-even chiral entity, the response remains constant with time-reversal operation as $R(I, B) = R(-I, -B)$. However, the system shows $R(I, B) \neq R(-I, B)$ as non-reciprocal resistance. In the case of eMChA, the enhancement of SOC by a factor of 100–1000 was observed again. It seems that such an enhancement is a common feature in chiral systems regardless of the time-reversal symmetry. It is notable that the coexistence of eMChA and CISS is also reported in molecular systems as well.[23]

4. Summary

Time-reversal symmetry is a very ambiguous term that can be easily misunderstood, as it encompasses several different meanings. Within the scope of fundamental equations in physics, such as the Schrodinger, Dirac, and Maxwell's equations, all are symmetric with respect to time-reversal, and the only asymmetry in time appears in the second law of thermodynamics (and the observation process in quantum mechanics). It is, however, common in solid-state physics to say that "time-reversal symmetry is broken" when a magnetic field is applied, but this statement refers to a situation where the source of the magnetic field is external to the system. If the source of the magnetic field (such as an electromagnet) is also time-reversed, it is difficult to say that symmetry is broken only by the magnetic field.

When discussing chirality and time-reversal symmetry, it is essential to clearly define what constitutes the system and what constitutes the field, as misunderstandings in these definitions can lead to confusion.[13,14] In this paper, the author has examined time-reversal symmetry as a property of the base to describe the system. The conversion from G_0 to M_0 likely requires dissipation and non-equilibrium conditions, introducing the second law of thermodynamics. Thus, when considering such processes, it is possible that the meaning of time-reversal symmetry could become doubly layered. The first layer is for $\mathcal{T}$-odd/ $\mathcal{T}$-even chirality and the second layer is about thermodynamic time reversal. In the CISS(II) process, these two kinds of time-reversal symmetry breaking are entangled.

Before the discovery of the CISS effect, it was generally assumed that both the spin and orbital degrees of freedom of electrons in closed-shell molecules were inactive. However, the CISS effect suggests that the dynamics of chiral molecules and crystals can generate magnetic seeds that involve the breaking of time-reversal symmetry. This will provide a new opportunity for the chiral materials to be used in spintronics. Although the CISS effect was originally discovered in a unique system of self-assembled monolayers on metal substrates using DNA or polypeptides, it has been extended to bulk crystal systems now, allowing for the application of solid-state physics experimental techniques and theories. There is still no consensus on the microscopic theory of the CISS effect, and thus further understanding is expected to progress by comparing the theories and experiments of molecular systems and solid-state systems. At the same time, although it is not easy to decide whether the magnetization comes from orbital or spin angular momentum, all of the above experiments can be described by both CISS and the orbital Edelstein effect because both effects can have orbital contributions.[24] People in this field are also interested in the relationship between chiral phonon/vibration and spin angular momentum, which is a dynamic and mechanical aspect of the system.[25] Indeed, recent discovery of spin polarization detected by ISHE electrodes attached to a quartz under thermal gradient[26] suggests that truly chiral phonons[27] may be a carrier for spin polarization, although the detailed mechanism is not clear. In the case of $CrNb_3S_6$, chiral phonons and itinerant electrons may produce a combined quasi-particle that propagates a long distance.

In this short review, the author has pointed out the importance of G_0 to M_0 conversion, effectively enhanced SOC, and nonlocal spin detection in solid-state CISS. Mechanisms of these phenomena are still under discussion. Establishing clear experimental criteria to distinguish $\mathcal{T}$-even and $\mathcal{T}$-broken CISS responses will be essential for developing a unified microscopic understanding of the CISS effect. Since the CISS effect not only is of interest for its potential application in spintronics and chiral electrochemistry (such as oxygen evolution and asymmetric synthesis reactions) but also seems to impact charge separation in biological systems and interactions between biomolecules, and those unknown aspects should be

understood to further develop our insights into nature. The author hopes that this paper will be of help for researchers across a broad range of fields, from condensed matter physics to life sciences, who are interested in the CISS effect.

Conflicts of interest

There are no conflicts to declare.

Data availability

No primary research results, software or code have been included and no new data were generated or analysed as part of this review.

Acknowledgements

This paper is based on collaborative research with Takuro Sato, Ryota Nakajima, Daichi Hirobe, Genta Kawaguchi, Yoji Nabei, Tetsuya Narushima, Hiromi Okamoto, Jun-ichiro Kishine, Hiroaki Kusunose, Akito Inui, Ryuya Aoki, Yuki Nishiue, Kohei Shiota, Yusuke Shimamoto, Yusuke Kousaka, Hiroaki Shishido, Masayuki Suda, Jun-ichiro Ohe, and Yoshihiko Togwa, to whom the author is deeply grateful. Those researches have been supported by JSPS (17H02923, 17H02767, 19K03751, 19H00891, 19K21039, 20K20903, 21H01032, 23H00291, 23H00091 and 24K01331), JST (JPMJPR20L9, JPMJER1301 and JPMJER2503), and the National Institutes of Natural Sciences (OML012301 and 23IMS1101), as well as by the MEXT Nano Platform, the ARIM Project, and the Equipment Development Center and Instrument Center at the Institute for Molecular Science. The author also thanks Takuya Sato and Yusuke Kato for fruitful discussions and valuable suggestions.

References

1 (*a*) B. P. Bloom, Y. Paltiel, R. Naaman and D. H. Waldeck, *Chem. Rev.*, 2024, **124**, 1950; (*b*) R. Naaman, Y. Paltiel and D. H. Waldeck, *Nat. Rev. Chem.*, 2019, **3**, 250; (*c*) P. C. Mondal, C. Fontanesi, D. H. Waldeck and R. Naaman, *Acc. Chem. Res.*, 2016, **49**, 2560.
2 B. Göhler, V. Hamelbeck, T. Z. Markus, M. Kettner, G. F. Hanne, Z. Vager, R. Naaman and H. Zacharias, *Science*, 2011, **331**, 894.
3 F. Evers, *et al.*, *Adv. Mater.*, 2022, **34**, 2106629.
4 R. Sala, S. K. Behera, A. R. Karmakar, M. Moioli, R. Martinazzo and M. Cococcioni, *Nanoscale*, 2026, DOI: 10.1039/D5NR04557F.
5 (*a*) V. M. Edelstein, *Solid State Commun.*, 1990, **73**, 233; (*b*) V. M. Edelstein, *Phys. Rev. Lett.*, 1995, **75**, 2004.
6 K. Banerjee-Ghosh, *et al.*, *Science*, 2018, **360**, 1331.
7 A. Kumar, *et al.*, *Proc. Nat. Acad. Sci. U. S. A.*, 2017, **114**, 2474.
8 S. Ghosh, S. Mishra, E. Avigad, B. P. Bloom, L. T. Baczewski, S. Yochelis, Y. Paltiel, R. Naaman and D. H. Waldeck, *J. Phys. Chem. Lett.*, 2020, **11**, 1550.
9 N. Sukenik, F. Tassinari, S. Yochelis, O. Millo, L. T. Baczewski and Y. Paltiel, *Molecules*, 2020, **25**, 6036.
10 O. B. Dor, S. Yochelis, A. Radko, K. Vankayala, E. Capua, A. Capua, S.-H. Yang, L. T. Baczewski, S. S. P. Parkin, R. Naaman and Y. Paltiel, *Nat. Commun.*, 2017, **8**, 14567.
11 I. Meirzada, N. Sukenik, G. Haim, S. Yochelis, L. T. Baczewski, Y. Paltiel and N. Bar-Gill, *ACS Nano*, 2021, **15**, 5574.
12 (*a*) L. D. Barron, *Chem. Soc. Rev.*, 1986, **15**, 189; (*b*) L. D. Barron, *Rend. Fis. Acc. Lincei*, 2013, **24**, 179.
13 J. Kishine, H. Kusunose and H. M. Yamamoto, *Isr. J. Chem.*, 2022, **62**, e2022000.
14 H. Kusunose, J. Kishine and H. M. Yamamoto, *Appl. Phys. Lett.*, 2024, **124**, 260501.
15 K. Yoshimi, Y. Kato, Y. Suzuki, S. Sumita, T. Sato, H. M. Yamamoto, Y. Togawa, H. Kusunose and J. Kishine, *Phys. Rev. B*, 2026, **113**, 155112.
16 C. Kulkarni, A. K. Mondal, T. K. Das, G. Grinbom, F. Tassinari, M. F. J. Mabesoone, E. W. Meijer and R. Naaman, *Adv. Mater.*, 2020, **32**, 1904965.
17 R. Nakajima, D. Hirobe, G. Kawaguchi, Y. Nabei, T. Sato, T. Narushima, H. Okamoto and H. M. Yamamoto, *Nature*, 2023, **613**, 479.
18 L. E. Vorob'ev, E. L. Ivchenko, G. E. Pikus, I. I. Farbshtein, V. A. Shalygin and A. V. Shturbin, *Pis'ma Zh. Eksp. Teor. Fiz.*, 1979, **29**, 485.
19 T. Furukawa, Y. Shimokawa, K. Kobayashi and T. Itou, *Nat. Commun.*, 2017, **8**, 954.
20 A. Inui, R. Aoki, Y. Nishiue, K. Shiota, Y. Kousaka, H. Shishido, D. Hirobe, M. Suda, J. Ohe, J. Kishine, H. M. Yamamoto and Y. Togawa, *Phys. Rev. Lett.*, 2020, **124**, 166602.
21 Y. Nabei, D. Hirobe, Y. Shimamoto, K. Shiota, A. Inui, Y. Kousaka, Y. Togawa and H. M. Yamamoto, *Appl. Phys. Lett.*, 2020, **117**, 052408.
22 T. Sato, H. Goto and H. M. Yamamoto, *Phys. Rev. Res.*, 2025, **7**, 023056.
23 A. Singh, K. Martin, M. M. Talamo, A. Houssin, N. Vanthuyne, N. Avarvari and O. Tal, *Nat. Commun.*, 2025, **16**, 1759.
24 (*a*) T. Yoda, T. Yokoyama and S. Murakami, *Sci. Rep.*, 2015, **5**, 12024; (*b*) Y. Liu, J. Xiao, J. Koo and B. Yan, *Nat. Mater*, 2021, **20**, 638.
25 (*a*) A. Kato, H. M. Yamamoto and J. Kishine, *Phys. Rev. B*, 2022, **105**, 195117; (*b*) J. Fransson, *Phys. Rev. B*, 2020, **102**, 235416; (*c*) H.-H. Teh, W. Dou and J. E. Subotnik, *Phys. Rev. B*, 2022, **106**, 184302.
26 K. Ohe, H. Shishido, M. Kato, S. Utsumi, H. Matsuura and Y. Togawa, *Phys. Rev. Lett.*, 2024, **132**, 056302.
27 K. Ishito, H. Mao, Y. Kousaka, Y. Togawa, S. Iwasaki, T. Zhang, S. Murakami, J. Kishine and T. Satoh, *Nat. Phys.*, 2023, **19**, 35.